Andrade rheology in planetary science

M. Walterová[1], A.-C. Plesa[1], F. W. Wagner[2], and D. Breuer[1]

[1]Institute of Planetary Research, German Aerospace Center (DLR), Berlin, Germany
[2]Jülich Supercomputing Center, Forschungszentrum Jülich (FZJ), Jülich, Germany

Key Points:

- We revisit the Andrade rheology and its empirical parameters commonly used for interpreting tidal measurements of terrestrial planets.
- Our analysis suggests that the Andrade parameters are mildly rigidity-dependent, and preferred parameter ranges are derived from data.
- Uncertainties in the Andrade parameters can affect the inversion of mantle viscosity by several orders of magnitude.

Corresponding author: Michaela Walterová, kanovami@gmail.com

Abstract

The anelastic reaction of planet-forming materials is successfully described by the Andrade rheological model, which presents an extension of the simple Maxwell rheology. In addition to the instantaneous elastic deformation and the long-term viscous creep, the Andrade rheology incorporates the transient creep in metals, ices, and silicates, and is able to explain the tidal parameters of planets even in cases, where the Maxwell model requires the assumption of unrealistically low mantle viscosities. In this work, we discuss the applications of the Andrade model in planetary science, the parameters used in the literature, and their justification by material science and geodesy. We also examine the topic of relating the empirical tidal parameters to the mantle viscosity of moons and terrestrial planets and assess the limitations resulting from the uncertainties in the rheological parameters. Our study illustrates the necessity for future measurements that would help to better calibrate the rheological models to conditions relevant to the deep interiors of planets and moons.

Plain Language Summary

The interior structure of most planets and moons can only be studied by indirect methods, for example by measuring the global deformations caused by the uneven gravitational force acting throughout the body. At the same time, to find out how global deformation relates to the interior structure, we need to understand the properties of planet-forming materials at high pressures and temperatures. In this work, we discuss a frequently used model (the Andrade model) that successfully describes the relationship between stress and deformation observed in many kinds of materials. We review the parameters of this model, their values implied by laboratory measurements, and the effect of our limited knowledge on the reconstruction of celestial bodies' interior structures. Finally, we also propose future measurements that may help to reduce the uncertainties of the interior structure estimation.

1 Andrade model and its parameters

Andrade (1910) introduced an empirical model of the transient deformation in metal wires under constant stress, in which the extension of the wire scales with time t as $t^{1/3}$. His model contained the free parameter β, a quantity with the dimension of $\mathrm{s}^{-1/3}\ \mathrm{Pa}^{-1}$ that depends on the composition and microscopic properties of the sample as well as on the laboratory conditions (temperature and pressure). In later studies (e.g., Jackson, 2000), the exponent in the time dependence (1/3) was replaced by a new free parameter α, the value of which lies between 0 and 1. Here, we will call this parameterization "the $\alpha-\beta$ approach".

Almost a century later, Castillo-Rogez et al. (2011) and Efroimsky (2012a, 2012b) established a second parameterization. They realized that the fractional dimension of β might hinder the physical meaning of the Andrade model and that the parameter should be rather expressed as a combination of other quantities, namely the rigidity μ and viscosity η, or the Maxwell time $\tau_\mathrm{M} = \eta/\mu$. Castillo-Rogez et al. (2011) found that:

$$\beta \approx \mu^{-1}\tau_\mathrm{M}^{-\alpha} = \mu^{-(1-\alpha)}\eta^{-\alpha} \tag{1}$$

and Efroimsky (2012a, 2012b) further generalised this expression by introducing the Andrade time τ_A and a dimensionless parameter time $\zeta = \tau_\mathrm{A}/\tau_\mathrm{M}$. The value of β can then be related to the other parameters through:

$$\beta = \mu^{-1}(\zeta\,\tau_\mathrm{M})^{-\alpha} = \mu^{-1}\tau_\mathrm{A}^{-\alpha}\ . \tag{2}$$

We will call this parameterization "the $\alpha-\zeta$ approach".

The following two subsections provide a historical overview of Andrade rheology and its applications in material science and geophysics. In Section 2, we discuss the values of parameters α, β, and ζ implied by laboratory studies under high pressures and we illustrate how the uncertainty in Andrade parameters, together with the uncertainty in tidal measurements, affects the inference of terrestrial planets' mantle viscosities. The results are further reviewed in Section 3 and summarized in the Conclusions (Section 4).

1.1 The α–β parameterisation

The historically older α–β approach dates back to the pioneering work of E. N. da Costa Andrade (Andrade, 1910). Andrade (1910) measured the lengthening of metal wires (Pb, Pb+Al, Cu) under constant tensile stresses and at constant temperatures and noticed that the extension of a wire can be generally divided into three parts: *(a)* the immediate elastic reaction, *(b)* an initial transient creep, later called the β-flow, and *(c)* the steady-state viscous creep. Specifically, the contribution of the transient creep with respect to the viscous creep depended on the wire's composition and on temperature. After fitting the lengthening of the metal wires with various functions, Andrade found that the relation:

$$l = l_0 \left(1 + \beta t^{1/3}\right) e^{\kappa t} \,, \tag{3}$$

where l is the length at time t, l_0 is the initial length, and κ is a fitted parameter, gives the most accurate results for the initial transient part of the deformation. Filtering out the contribution of the steady-state viscous flow, the transient deformation caused by the material's anelasticity reads as:

$$\Delta l / l_0 = \beta t^{1/3} \,; \tag{4}$$

hence, its time dependence is given by the parameter β and by the exponent 1/3.

The exponential factor in equation (3) was introduced by Andrade (1910) to account for the increase of the wire's gauge length with extension. Cottrell and Aytekin (1947), who performed experiments with zinc wires under constant stress, chose instead to evaluate the shear strain γ in their samples and rewrote Andrade's formula to a form similar to what is nowadays commonly used in planetary science and rheological experiments:

$$\gamma(t) = \gamma_0 + \beta t^{1/3} + \kappa t \,. \tag{5}$$

Note that κ is a measure of viscosity rescaled by the applied (constant) stress and, similarly, γ_0 is equal to a rescaled inverse rigidity.

An interesting feature of the Andrade model, pointed out already by the contemporaries of Andrade and still remaining a mystery, is its applicability not only to metals and polycrystalline solids, but also to amorphous materials: the same power-law time dependence of the transient creep was found in experiments with celluloid (Filon & Jessop, 1923), colloidal glass (Siebenbürger et al., 2012), asphalt (Saal & Labout, 1940), mortar (Bingham & Reiner, 1933), rubber (Braun, 1936), and even with flour dough (Schofield & Scott Blair, 1933; Henderson, 1951). While the exponent 1/3 was most widely and successfully used for fitting the creep curves, Kennedy (1953) also discusses the applicability of a general power law βt^p for fitting both the steady-state creep and the transient creep at once, and lists the values of p obtained by several other authors. When corrected for the contribution of the steady-state creep, the values summarised by Kennedy (1953) typically fall between $p = 0.3$ and $p = 0.4$. A larger deviation was only reported for carbon steel (with $p = 0.18$ or $p = 0.47$; Johnson, 1941) and macerated fabric-filled phenoplast ($p = 0.50$; Gailus & Telfair, 1945).

Along with the experimental studies of the high-temperature creep, the time dependence of deformation was also investigated for large-scale geophysical phenomena. Jeffreys (1958) introduced the "modified Lomnitz law" and attempted to fit the attenuation of seismic waves, tidal waves, and free oscillations by a single creep law, inspired by the Andrade's empirical law with the shear strain linked to time as $\gamma \propto t^{1/3}$. The creep law of Jeffreys reads as:

$$\gamma(t) = \frac{\sigma}{\mu}\left[1 + \frac{q}{\alpha}\left\{(1+at)^{\alpha} - 1\right\}\right] , \tag{6}$$

where σ is the shear stress, μ the unrelaxed rigidity, and a, q symbolize additional constants, related to the Maxwell time. To our knowledge, this is the first occurrence of the notation α in an Andrade-type law. Regarding the two additional constants, a is reported to be of the order of 10^3 and q is small, between 10^{-3} and 10^{-2} (Jeffreys, 1958). Jeffreys applied his creep law to a wide range of geophysical phenomena, ranging from seismology to the rotational and orbital dynamics of planetary satellites. Specifically, for tidal friction and free nutation, Jeffreys and Crampin (1960) proposed the following approximation, valid for $at \gg 1$:

$$\gamma(t) = \frac{\sigma}{\mu}\left[1 + \frac{q}{\alpha}a^{\alpha}t^{\alpha}\right] . \tag{7}$$

While in the initial works on creep in the Earth and planets Jeffreys derived $\alpha = 0.17$, a correction published in Jeffreys and Crampin (1960) includes a value $\alpha = 0.25$, which is much closer to the original Andrade's exponent. Later derivation, comparing the attenuation of seismic shear waves and the attenuation of Earth's free nutation, yielded α between 0.14 and 0.21, with 0.19 being the preferred value (Jeffreys, 1972).

So far, we have mostly discussed the transient component of the strain which is measured in creep experiments when studying the lengthening of a wire under constant tensile stress. The strain was thus expressed in the time domain. However, for a range of geophysically-relevant applications—and also for torsion oscillation experiments—it is more convenient to express the quantities in the frequency domain. If we rewrite equation (5) to a modern form (e.g., Jackson et al., 2002),

$$J(t) = J_{\mathrm{U}} + \beta t^{\alpha} + \frac{t}{\eta} , \tag{8}$$

with $J(t)$ being the creep function (strain resulting from a step-function stress), $J_{\mathrm{U}} = 1/\mu$ being the unrelaxed compliance related to the unrelaxed rigidity μ, and η symbolizing the viscosity, we can transition to the frequency domain by taking a Laplace transform of (8). This leads then to the following equation:

$$\bar{J}(\omega) = J_{\mathrm{U}} - \frac{\mathrm{i}}{\eta\omega} + \beta(\mathrm{i}\omega)^{-\alpha}\,\Gamma(1+\alpha) , \tag{9}$$

where $\bar{J}(\omega)$ is now called the dynamic compliance, i is the imaginary unit, ω is the angular frequency, and Γ the gamma function. If we introduce the Maxwell time $\tau_{\mathrm{M}} = \eta/\mu$ and the new parameter $\beta^* = \beta\mu$, we can also write equation (9) as (Jackson & Faul, 2010):

$$\bar{J}(\omega) = J_{\mathrm{U}}\left\{1 - \frac{\mathrm{i}}{\tau_{\mathrm{M}}\omega} + \beta^*(\mathrm{i}\omega)^{-\alpha}\,\Gamma(1+\alpha)\right\} . \tag{10}$$

Regarding the dependence of the above rheological laws on laboratory conditions or on the conditions of deep Earth interior, it has been long known (e.g., Kê, 1947; Dorn, 1955; Kennedy, 1956; Anderson & Minster, 1979) that both transient creep and steady-state creep are thermally-activated processes and follow the Arrhenian temperature dependence. Kê (1947) used an exponential factor to rescale measurements of creep in an

aluminum sample subjected to constant stress at different temperatures, and, identically, Dorn (1955) showed that the creep curves corresponding to different temperatures overlap each other when using a "compensated time", or time multiplied by the Arrhenian factor $\exp\{-H^*/RT\}$, where H^* is the activation enthalpy, R the universal gas constant, and T the temperature.

To fit the temperature, pressure, and grain-size dependence of both the energy dissipation and modulus dispersion ($\bar{\mu}(\omega) = 1/\bar{J}(\omega)$) of individual mineral specimens, Jackson et al. (2004) introduced the pseudo-period master variable, which can be substituted for the actual period $2\pi/\omega$ in equations (9) and (10). The inverse of the pseudo-period, called the pseudo-frequency and inputted in place of the actual frequency ω in equations (9) and (10), reads as:

$$\omega_{\mathrm{B}} = \omega \left(\frac{d}{d_{\mathrm{R}}}\right)^{m} \exp\left\{\frac{E^*}{R}\left(\frac{1}{T} - \frac{1}{T_{\mathrm{R}}}\right)\right\} \exp\left\{\frac{V^*}{R}\left(\frac{P}{T} - \frac{P_{\mathrm{R}}}{T_{\mathrm{R}}}\right)\right\} . \tag{11}$$

In the above expression, E^* and V^* are the activation energy and volume, d_{R}, T_{R}, P_{R} denote the reference grain size, temperature, and pressure, respectively, d, T, P are the actual values of the grain size, temperature, and pressure, and m is the grain-size exponent.

For the sake of completeness, we note that the pseudo-frequency given by equation (11) implies a steady-state viscosity of the form:

$$\eta = \eta_{\mathrm{R}} \left(\frac{d}{d_{\mathrm{R}}}\right)^{m} \exp\left\{\frac{E^*}{R}\left(\frac{1}{T} - \frac{1}{T_{\mathrm{R}}}\right)\right\} \exp\left\{\frac{V^*}{R}\left(\frac{P}{T} - \frac{P_{\mathrm{R}}}{T_{\mathrm{R}}}\right)\right\} , \tag{12}$$

where η_{R} is the reference viscosity corresponding to the reference laboratory conditions. Similarly, the implied scaling of the Andrade parameter β is:

$$\beta = \beta_{\mathrm{R}} \left(\frac{d}{d_{\mathrm{R}}}\right)^{-\alpha m} \exp\left\{-\frac{\alpha E^*}{R}\left(\frac{1}{T} - \frac{1}{T_{\mathrm{R}}}\right)\right\} \exp\left\{-\frac{\alpha V^*}{R}\left(\frac{P}{T} - \frac{P_{\mathrm{R}}}{T_{\mathrm{R}}}\right)\right\} , \tag{13}$$

with β_{R} denoting the reference value.

1.2 The α–ζ parameterisation

As mentioned in the introduction to this section, the motivation for a reparameterisation of the transient response described by Andrade (1910) stems from the dimensional analysis. The dimension of the empirical parameter β is $\mathrm{s}^{-\alpha}\ \mathrm{Pa}^{-1}$, i.e., it contains a fractional power of the unit of time. Moreover, apart from scaling the shear strain produced by transient creep relative to the elastic and viscous strain, it lacks a clear physical interpretation.

Castillo-Rogez et al. (2011) discovered that β can be related to the viscosity and rigidity of a sample, and used the empirical data given by Tan et al. (2001) and Jackson et al. (2002) to seek the slope of the proportionality $\beta \propto \mu^{\alpha-1}/\eta^{\alpha}$. The slope was found to be close to unity, although, as Castillo-Rogez et al. (2011) note, the R-squared value for the dataset of Tan et al. (2001) is only 0.39, meaning that only 40% of data was explained by the proposed relation. A further generalization of the proportionality found in empirical data was introduced by Efroimsky (2012a, 2012b), who defined the "Andrade time" τ_{A} as a characteristic timescale of Andrade's transient creep and the parameter ζ as the ratio between the Andrade and Maxwell times:

$$\tau_{\mathrm{A}} = (\beta^*)^{-1/\alpha} , \qquad \zeta = \frac{\tau_{\mathrm{A}}}{\tau_{\mathrm{M}}} = \frac{\mu}{\eta(\beta^*)^{1/\alpha}} . \tag{14}$$

The dynamic compliance of the Andrade model, rewritten in terms of the old parameter α and the new parameter ζ, is given by Efroimsky (2012a, 2012b) as:

$$\bar{J}(\omega) = \frac{1}{\mu} - \frac{\mathrm{i}}{\eta\omega} + \frac{\mu^{\alpha-1}}{(\mathrm{i}\zeta\eta\omega)^{\alpha}}\,\Gamma(1+\alpha)\,. \tag{15}$$

For the sake of completeness, we also write down the relation between the original parameter β and the new parameter ζ, which is:

$$\beta = \frac{\mu^{\alpha-1}}{(\zeta\eta)^{\alpha}}. \tag{16}$$

In the α–β approach of Jackson and Faul (2010), both η and β are endowed with an implied temperature, pressure, and grain-size dependence that is included in the pseudo-frequency. On the other hand, thanks to its definition in equation (14), ζ does not explicitly depend on these parameters, as long as the same pseudo-frequency (equation (11)) in the dynamic compliance of the α–β approach applies to both the transient and the steady-state term. Theoretically, this is not always the case and as noted in various works (e.g., Hirth & Kohlstedt, 2003; Jackson & Faul, 2010), at least the grain-size exponent seems to be different between the two terms, with steady-state creep preferring $m = 3$ (Hirth & Kohlstedt, 2003) and transient creep exhibiting lower values, e.g., $m = 1.31$ (Jackson & Faul, 2010). As a consequence, the parameter ζ might be a function of the grain size. In principle, the activation volumes and energies of the two components of the creep law can also deviate from those implied by the pseudo-frequency fit and ζ may then depend on the temperature, pressure, and mineralogical composition of the sample.

2 Datasets and uncertainties

2.1 Andrade parameters implied by the existing datasets

Although the literature addressing rheological experiments with planet-forming materials is relatively rich, only a limited number of papers provide Andrade-type fits to the experimental data. More widespread is the fitting of the frequency-dependent attenuation of seismic waves in a viscoelastic medium, parameterized by the inverse quality factor Q^{-1}, with a power law $Q^{-1} \approx \omega^{-p}$, where p is an exponent generally different from the Andrade parameter α (Gribb & Cooper, 1998). The power law fits the contributions of both the transient creep and the viscous creep in a given frequency range with a single exponent. Therefore, we should expect $\alpha < p$. Only for low levels of anelastic dissipation and even weaker levels of viscous dissipation is the power law exponent equal to α (Bagheri et al., 2022).

A comprehensive overview of mineralogical, geodetical, and seismologic literature dealing with the power-law frequency dependence of attenuation was given by Efroimsky and Lainey (2007), and the authors also focused on the power law's implications for the modeling of tidal effects in viscoelastic planets. Values of p in laboratory studies at the transient-creep portion of the dissipation spectrum range between $0.1-0.4$ (e.g., Berckhemer et al., 1982; Gueguen et al., 1989; Karato & Spetzler, 1990; Tan et al., 1997; Gribb & Cooper, 1998; Tan et al., 2001). Similar, or even lower values are indicated by the observation of geophysical processes such as the attenuation of Chandler wobble, free nutations, tidal waves, and seismic waves (e.g., Smith & Dahlen, 1981; Anderson & Minster, 1979; Anderson & Given, 1982; Lau & Faul, 2019).

Apart from the power-law fit, multiple laboratory studies and some of the recent inversions of geophysical data of terrestrial planets (e.g., Bagheri et al., 2019; Xiao et al., 2022) seek for the parameters of the Andrade law. In the overview below, we specif-

ically focus on the results reported by the Australian National University (ANU) laboratory that are most often adopted in models of tidal deformation of terrestrial planets. Their tests were performed under the confining pressure of 200 MPa; however, as indicated by the 5 GPa experiments of Li and Weidner (2007), the same frequency dependence of viscoelastic effects might also be expected at higher pressures. We review the Andrade parameters α and ζ as well as the Maxwell and Andrade timescales (τ_{M}, τ_{A}) provided in the cited papers or obtained by fitting the raw data. Parameters ζ and τ_{A} are calculated from relations given in equation (14).

The form of the Andrade law used for fitting laboratory measurements corresponds to the original $\alpha-\beta$ approach, and the quantities measured in the torsional oscillation or microcreep experiments are the frequency-dependent modulus of complex rigidity (also called shear modulus, e.g., Jackson et al., 2004):

$$|\bar{\mu}(\omega)| = \left[\mathrm{Re}\{\bar{J}(\omega)\}^2 + \mathrm{Im}\{\bar{J}(\omega)\}^2\right]^{-\frac{1}{2}} \tag{17}$$

and the inverse quality factor (or "internal friction"):

$$Q^{-1}(\omega) = \frac{\mathrm{Im}\{\bar{J}(\omega)\}}{\mathrm{Re}\{\bar{J}(\omega)\}} \tag{18}$$

Tan et al. (2001) studied three samples of fine-grained and essentially melt-free polycrystalline olivine under a confining pressure of 200 MPa. The pressed samples were heated to 1300 °C for several hours and then slowly cooled down to room temperature, with mechanical testing performed in temperature intervals of 100 °C and in the period range 1−100 s. The prior high-temperature annealing, slow cooling, as well as relatively small grain sizes (8−150 μm), helped to prevent microcracking in the specimens and to only concentrate on deformation produced by grain-boundary processes. At temperatures above 1000 °C, the samples manifested ongoing viscoelastic deformation, marked by unrelaxed rigidity reduction and dissipation increase with temperature and loading period.

The authors either fitted the data with the Andrade model in the time domain (for microcreep tests) or in the frequency domain (for torsional oscillation tests). Their parameter α lies between 0.07−0.36 for the torsional oscillation data and between 0.31−0.44 for the microcreep data. According to Tan et al. (2001), the former method is more direct and its results should be considered more robust than the fits to the latter method. From the Andrade parameter β, which is in the order of 10^{-13}−$10^{-11}\,\mathrm{s}^{-\alpha}\,\mathrm{Pa}^{-1}$ (or β^* between $0.01-0.8\,\mathrm{s}^{-\alpha}$), and from the fitted viscosities and rigidities, we can estimate the dimensionless parameter ζ as $0.03-25.52$ for microcreep and $0.17-33.23$ for torsion oscillations. Additionally, two torsion oscillation measurements of specimen 6261 at 1000 °C show extremely high values of ζ greater than 10^6, corresponding to the two smallest reported α. This peculiar result can be inspected along with Figure 9b of Tan et al. (2001), where the curve fitted to the 1000 °C data exhibits a slope different from the other cases. Although these two data points might be outliers, we still use them in our analysis at the end of this section.

Motivated by understanding the grain-size dependence of viscoelastic deformation, Jackson et al. (2002) investigated the attenuation in four samples of melt-free olivine polycrystals from both natural and synthetic precursors with mean grain radii d between 3−23 μm. The testing was performed under the same conditions as in Tan et al. (2001). In the temperature range $T \in [1000, 1200]$ °C or up to 1300 °C and in the period range $[1, 100]$ s, the authors found that the internal friction can be represented by a mild power-law dependence not only on the frequency but also on the grain size. In the best-fitting model, both quantities were endowed with the same exponent. Jackson et al. (2002) also adopted the Arrhenian rescaling of frequency used previously by Kê (1947).

Identically to the datasets of Tan et al. (2001), the values of the Andrade parameter β reported by Jackson et al. (2002) are in the range $10^{-13}-10^{-11}\mathrm{Pa}^{-1}\,\mathrm{s}^{-\alpha}$ for rigidities of $47-64\,\mathrm{GPa}$ and viscosities of $10^{12}-10^{14}\,\mathrm{Pa\,s}$. This corresponds to $\beta^* = 0.009-0.45\,\mathrm{s}^{-\alpha}$. From the second equation of (14), we find that within the $\alpha-\zeta$ parameterization, the data of Jackson et al. (2002) require ζ lying between 0.14 and 47, with a preference for the lower values. The values of α are between $0.18 - 0.62$, with the higher values ($\alpha > 0.3$) typically resulting from the microcreep data processing.

The datasets of Tan et al. (2001) and Jackson et al. (2002) were further analysed by Castillo-Rogez et al. (2011), who found that the slope of β as a function of $\eta^{-\alpha}\mu^{-(1-\alpha)}$ should be close to one, which would imply a mean value of $\zeta \sim 1$. We will reconstruct the analysis of Castillo-Rogez et al. (2011) later in this section, using three additional datasets.

Jackson et al. (2004) extended the previous studies by including dissipation in melt-bearing specimens as well and fitted the microcreep and torsional oscillation data with the Andrade model combined with a broad Gaussian peak. In this case, the polycrystalline samples, fabricated from natural and synthetic precursors, had grain sizes between 6.5 and $52.3\,\mu\mathrm{m}$ and a basaltic melt fraction up to 4%; the experimental conditions being the same as in the previous papers. For the Andrade portion of the fit to the microcreep data, we again see β in the range from 10^{-13} to $10^{-11}\mathrm{Pa}^{-1}\,\mathrm{s}^{-\alpha}$, corresponding now to $\beta^* = 0.04-1.38\,\mathrm{s}^{-\alpha}$. Interestingly, α follows a weakly negative trend with temperature: between 1000 and 1300°C, it slowly decreases from 0.4 to 0.29. The values of ζ fall between 0.03 and 4; i.e., they are typically one order of magnitude smaller than in the previous data set. The torsional oscillation data were fitted by Jackson et al. (2004) with a global pseudo-period Andrade model, and the resulting "global" α values are between 0.22 and 0.36.

Similarly, the global pseudo-period Andrade fit was applied to characterize the temperature dependence of viscoelastic dissipation and modulus dispersion in a new, particularly fine-grained ($d = 3\,\mu\mathrm{m}$) polycrystalline olivine sample of Jackson and Faul (2010). In the temperature range of $800-1200\,^\circ\mathrm{C}$ and the period range of $1-1000\,\mathrm{s}$, the authors found that the optimal Andrade parameters of the global fit are $\alpha = 0.33$ and $\beta^*_\mathrm{R} = 0.02\,\mathrm{s}^{-\alpha}$ (or $\beta_\mathrm{R} \approx 10^{-13}\,\mathrm{Pa}^{-1}\,\mathrm{s}^{-\alpha}$). The corresponding "reference" value of ζ at $T = 900\,^\circ\mathrm{C}$ and $P = 200\,\mathrm{MPa}$ would then be $\zeta_\mathrm{R} = 0.7$. This result is often adopted in the studies of tidal deformation in terrestrial planets (e.g., Padovan et al., 2014; Plesa et al., 2018; Steinbrügge et al., 2018; Bagheri et al., 2019), and the fitted temperature-dependence of the pseudo-frequency is typically complemented with a theoretical grain-size dependence (e.g., Hirth & Kohlstedt, 2003). However, one should keep in mind that this global fit is only based on the measurement of viscoelastic deformation in a single specimen of pure dry olivine, which is essentially melt-free and devoid of intragranular defects. The response of actual planetary mantles might be different.

In later works of the ANU laboratory devoted to the torsional oscillation studies of fine-grained olivine, the Andrade model was slowly abandoned in favor of the extended Burgers model. The extended Burgers model contains a finite-width absorption band in the relaxation spectrum, as opposed to the infinite-width absorption band that is implicitly present in the Andrade model, and is considered physically more transparent. Moreover, the choice of the alternative model was motivated by its greater flexibility in fitting data for melt-bearing samples and by the expectation of the existence of a high-frequency cut-off in the relaxation spectrum. The extended Burgers model has also been applied on several occasions to the inversions of geodetic data and used to infer the thermal state of terrestrial planets or the Moon (e.g., Nimmo et al., 2012; Nimmo & Faul, 2013; Khan et al., 2018; Bagheri et al., 2019).

Nevertheless, the Andrade model remains a popular choice for rheology in planetary science, especially for its parametric economy. Since the laboratory studies are focused on the rheological properties of mostly pure samples under specific laboratory con-

ditions, their results can inform the models of planetary interiors, but reconstructing the planetary interiors from geodetic observations might require much greater variability in the rheological parameters. From a practical point of view, the Andrade model requires the variation of a smaller number of parameters, and it is thus better suited for modelling planets with a limited number of observational constraints.

To explore the parameters of the Andrade model implied by newer datasets obtained with samples different from pure olivine, we analysed the processed data obtained and presented by Barnhoorn et al. (2016) and Qu et al. (2021). The data were originally fitted with the extended Burgers model; however, for the sake of the present study, we fitted them individually (for each temperature) as well as globally (using the pseudo-period master variable, for Qu et al., 2021) with the Andrade rheology within the $\alpha - \beta$ approach.

Barnhoorn et al. (2016) measured the viscoelastic deformation of polycrystalline MgO, which is the Mg-rich end-member of the lower-mantle mineral ferropericlase that might play the dominant role in the deformation of the lower mantle (Girard et al., 2016). A study of MgO was also presented by Webb and Jackson (2003); however, those earlier results, including an Andrade fit, were strongly affected by the presence of an unfitted dissipation peak in the spectrum. Barnhoorn et al. (2016) analysed four samples of MgO with grain sizes between $0.2-104\,\mu$m in a broad temperature interval of $20-1300\,^{\circ}$C and at the same pressures and loading periods as in the previous studies. For the smallest-grain sample, the forced oscillation experiments were only conducted at temperatures below $900\,^{\circ}$C and for the coarsest-grain sample, the data at high temperatures and long loading periods were likely affected by underestimated dissipation in a control specimen (Barnhoorn et al., 2016). For these reasons, we only fitted the Andrade model to the high-temperature data of the well-characterized sample 1077 (with $d = 8.8\,\mu$m) and to a few selected high-temperature measurements of the two samples with smaller grain sizes. Within the individual fits, we observe α between 0.20 and 0.42. The value is increasing monotonically with the temperature for each of the individual samples and the highest values ($\alpha > 0.3$) are found for the sample with the smallest grain size (studied at $T = 800-900\,^{\circ}$C). For β, we again find values between 10^{-13} and $10^{-12}\,\mathrm{Pa^{-1}\,s^{-\alpha}}$, corresponding to $\beta^* = 0.03 - 0.56\,\mathrm{s^{-\alpha}}$. Similarly to α, β^* is also increasing with temperature for each of the samples, and the smallest-grain sample shows $\beta^* < 0.1$. Parameter ζ attains values between 0.02 and 3.67 and its temperature dependence is negative.

Qu et al. (2021) studied the anelastic properties of olivine-orthopyroxene (Ol−Px) mixtures with different proportions of the two minerals at the standard confining pressure of 200 MPa and in the temperature range from $1300\,^{\circ}$C down to $400\,^{\circ}$C. One of the samples, with 5%Ol and 95%Px, was heated to a high temperature twice: in the "first cycle" to $1200\,^{\circ}$C and in the "second cycle" to $1300\,^{\circ}$C. This procedure ensured a smaller amount of microcracks in the second cycle. By fitting the available processed data of Qu et al. (2021) for each considered temperature with the Andrade model, we found values of α and ζ consistent with the results for pure olivine ($\alpha = 0.21 - 0.32$, $\zeta = 0.03 - 24.63$). The parameter β^* is between 0.07 and $0.24\,\mathrm{Pa^{-1}\,s^{-\alpha}}$. Additionally, we fitted all data collected at temperatures greater than $1100\,^{\circ}$C for each sample with the pseudo-period Andrade model of Jackson and Faul (2010), considering the Arrhenian temperature dependence of viscoelastic deformation. The results of the global fit are listed in Table 1.

For all references listing the parameters of the individual Andrade-type fits to the experimental data (Tan et al., 2001; Jackson et al., 2002, 2004), as well as for our fits to the dataset of Barnhoorn et al. (2016) and Qu et al. (2021), we also explored possible correlations in the datasets. Figure 1 shows the Andrade parameters of olivine and Ol-Px mixtures as a function of the unrelaxed sample rigidity and distinguishes between fits obtained with the microcreep measurements (marked by triangles) and fits obtained

Param.	Unit	95Ol, 5Px	70Ol, 30Px	5Ol, 95Px (1)	5Ol, 95Px (2)
α	—	0.22	0.22	0.24	0.22
β^*_{R}	$\mathrm{s}^{-\alpha}$	0.006	0.01	0.009	0.008
ζ_{R}	—	0.46	1.92	0.92	0.36
η_{R}	Pa s	$10^{20.9}$	$10^{19.4}$	$10^{19.2}$	$10^{20.9}$
μ_{R}	GPa	61.3	59.7	49.9	63.8
E^*	kJ/mol	676	634	576	673
V^*	cm^3/mol	9.85	2.11	10.0	0

Table 1. Pseudo-period Andrade fit to the Ol-Px dataset of Qu et al. (2021). Subscript "R" indicates reference values at $T_{\mathrm{R}} = 900\,^{\circ}\mathrm{C}$ and $P_{\mathrm{R}} = 200\,\mathrm{MPa}$. The temperature dependence of unrelaxed rigidity was modelled as $\mu(T) = \mu_{\mathrm{R}} + (T - T_{\mathrm{R}})\frac{\partial \mu}{\partial T}$ with $\frac{\partial \mu}{\partial T} = -13.6\,\mathrm{MPa}/^{\circ}\mathrm{C}$ (Bass, 1995; Jackson & Faul, 2010).

with the torsional oscillation measurements (marked by circles). As can be seen in Figure 1a, the microcreep fits tend to overestimate the value of α with respect to the torsional oscillation fits. This is a result of the microcreep data processing reported by Tan et al. (2001). There is also a weak indication for a trend in the Andrade parameters with increasing rigidity, with ζ preferring slightly higher values at higher μ. If this trend proves to be real, it would mean that the characteristic time scale of anelastic deformation in mantles of large terrestrial planets (e.g., Venus, Earth, and massive rocky exoplanets) is longer than the characteristic time scale of viscoelastic deformation (the Maxwell time). In that case, viscoelastic deformation would play a more important role in their tidal deformation than anelasticity (see also Efroimsky, 2012a). Figure 1 also contains two data points with unusually high ζ. As was discussed above, upon the inspection of Figure 9b of Tan et al. (2001), we tentatively consider those two data points outliers. The data for MgO are not depicted in the figure due to the considerably different range of sampled rigidities ($\mu = 78{-}146\,\mathrm{GPa}$). For MgO, ζ is mildly increasing and α is mildly decreasing with increasing rigidity for each of the samples individually, which might be an indication of a similar temperature dependence of these parameters and μ. However, we do not see any global trend.

Figure 2 compares the Andrade times calculated using expression (14) and the Maxwell times of polycrystalline olivine, MgO, and Ol-Px datasets. Most plotted data points, with the exception of the two suspected outliers, lie between the dashed lines indicating $\zeta = 0.1$ and $\zeta = 10$, and all values are confined to the interval $\zeta \in [0.01, 100]$.

Finally, Figure 3 shows a variation on Figure 4 of Castillo-Rogez et al. (2011), including not only the datasets of Tan et al. (2001) and Jackson et al. (2002) used in the original work but also the dataset of Jackson et al. (2004), which contains samples with small fractions of melt, and our fits to the individual samples of Barnhoorn et al. (2016) and Qu et al. (2021). The dashed line in the figure also shows a linear fit to the presented data, characterized by the equation below the data points.

In summary, the high-temperature and high-pressure forced oscillation studies of viscoelastic and anelastic effects in fine-grained polycrystalline olivine, Ol-Px mixtures, and MgO typically show ζ between 0.01 and 100, α between 0.15 and 0.4 (with a preference for $\alpha = 0.2 - 0.3$), and β^* between 0.006 and $1.38\,\mathrm{s}^{-\alpha}$. The linear fit to β as a function of $\eta^{-\alpha}\mu^{-(1-\alpha)}$, similar to that of Castillo-Rogez et al. (2011), has a slope $\zeta^{\alpha} = 0.42$ for all considered data, and $\zeta^{\alpha} = 0.54$ for melt-free olivine only, indicating a preference for $\zeta < 1$. In the next section, we will discuss how the uncertainties in the two Andrade parameters within the $\alpha{-}\zeta$ approach affect the determination of mantle viscosity in terrestrial planets.

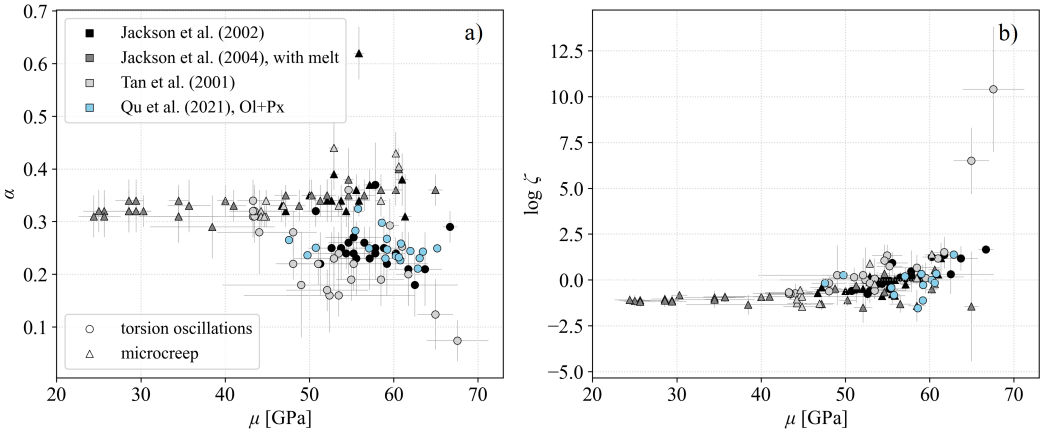

Figure 1. The Andrade parameters α *(a)* and ζ *(b)* as a function of unrelaxed sample rigidity for fine-grained polycrystalline olivine (gray) and olivine-pyroxene mixtures (light blue). Marker shapes indicate different measurement techniques: torsion oscillations (circles) vs. microcreep (triangles). The data points are obtained from individual fits to the frequency-dependent dissipation and modulus dispersion data collected at each temperature.

2.2 Consequences of uncertainties in the Andrade parameters

To investigate how the uncertainties on the Andrade parameters α and ζ affect the efforts to constrain the rheology of terrestrial planets, we explored the mantle viscosities implied by the real part of the tidal Love number k_2 reported in the literature. With the exception of one specific case, we assumed a fully liquid core of a prescribed size, an elastic structure of the mantle given either by a rescaled PREM (for Venus, Mars, and Mercury; Dziewonski & Anderson, 1981) or VPREMOON (for the Moon; Garcia et al., 2011), and we calculated the corresponding effective tidal viscosity of the mantle for different pairs of (α, ζ). For the sake of simplicity, the viscosity was considered constant in the entire mantle. The density of the core was always set to a constant value required to match the total planetary mass.

We emphasize that our intention in this section is only to illustrate the effect of the unknown Andrade parameters on the inferred mantle viscosity, and not to propose any conclusive mantle viscosity estimates for the planets. In reality, when reconstructing the interior structure of a planet, the core size is also inferred from the tidal deformation and should not be independent of the considered rheological model. Moreover, the mineralogy of the Martian, Cytherean ("Venusian"), and Mercurian mantle is likely different from that of the Earth, and the interior structure of Mars and the Moon is further constrained by other tidal parameters, such as the quality factor Q and the Love numbers h_2 and k_3.

For Venus, we considered a core radius of 3147 km, which is the best-fitting solution found by O'Neill (2021) for an Earth-like core composition. The degree-2 potential tidal Love number of Venus at the semi-diurnal frequency ($\omega = 1.25 \times 10^{-6}$ rad s^{-1}) is $k_2 = 0.295 \pm 0.066$ (Konopliv & Yoder, 1996). For the lower bound of the $2-\sigma$ interval of the Cytherean k_2, we did not find any fitting mantle viscosity for the model with a fully liquid core. This is in accordance with the results of Dumoulin et al. (2017), who showed that a k_2 value lower than 0.27 would indicate that the Cytherean core is fully solid. Therefore, in the particular case of Venus with $k_2 = 0.229$ (Figure 5), we modeled the core as fully solid, decribed by the viscoelastic Maxwell model, and we set its viscosity to $\eta_{\text{core}} = 10^{17}$ Pa s and its rigidity to $\mu_{\text{core}} = 150$ GPa. The core radius pre-

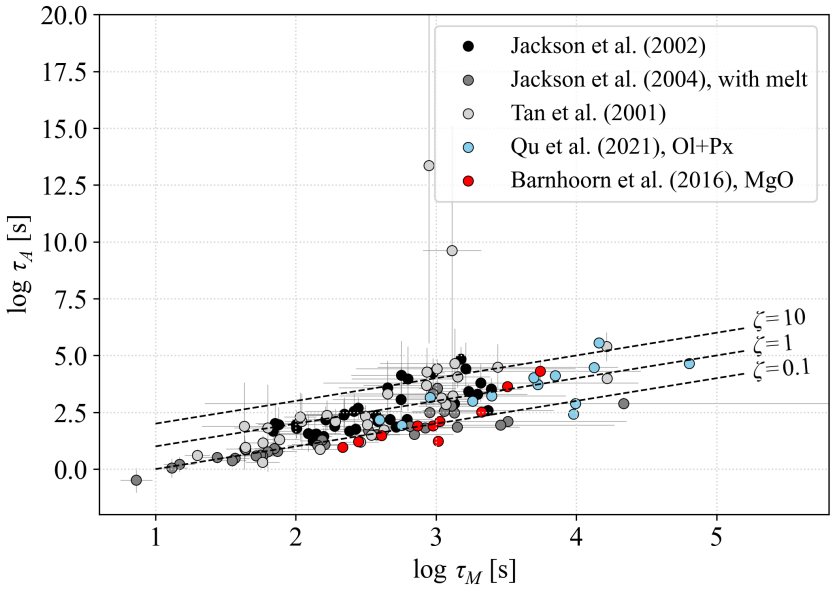

Figure 2. The Andrade time τ_A compared to the Maxwell time τ_M for polycrystalline olivine, MgO, and Ol-Px mixtures. Dashed lines indicate different values of the "relative Andrade time" (the parameter ζ).

scribed for Mars was 1830 km (Stähler et al., 2021), with the Love number at the semi-diurnal frequency ($\omega = 1.42 \times 10^{-4}$ rad s^{-1}) being $k_2 = 0.174 \pm 0.008$ (Konopliv et al., 2020). Mercury's core radius was set to 1955 km, which is the mean value found by Goossens et al. (2022) for the Love number $k_2 = 0.569 \pm 0.025$ estimated by Genova et al. (2019) at the annual loading frequency ($\omega = 8.26 \times 10^{-7}$ rad s^{-1}). Finally, for the Moon, we considered a core radius of 380 km (Garcia et al., 2011) and the Love number at the monthly frequency ($\omega = 2.67 \times 10^{-6}$ rad s^{-1}) equal to $k_2 = 0.02422 \pm 0.00022$ (Williams et al., 2014).

Figure 4 shows the results of our analysis, where we fitted the mean value of k_2 reported for each of the planets. Similarly, Figures 5 and 6 show the results of the same analysis for the lower and the upper bound of the reported intervals of k_2. The intervals are $2-\sigma$ for Venus but potentially larger for Mercury, Mars, and the Moon, where the error bars are artificially widened to account for all possible sources of uncertainty.

The difference between the individual levels of the contour plots in all three figures is one order of magnitude, which enables us to readily estimate the effect of varying α and ζ on the inferred mantle viscosity, assuming that the core size is known (e.g., from the moment of inertia, mineralogical considerations, or seismic measurements). The horizontal solid bars indicate the range of α most often found in the literature (as discussed in the previous section) for two values of ζ. The first one, $\zeta = 1$, is an assumption often used in the studies of planetary interiors (e.g., Castillo-Rogez et al., 2011; Běhounková et al., 2013; Dumoulin et al., 2017; Goossens et al., 2022; Xiao et al., 2022). The second one, $\zeta = 0.1$, is approximately equal to the value of ζ corresponding to the slope of the linear fit in our Figure 3.

Additionally, the thin white isolines in Figure 4 also show the tidal quality factor Q predicted for each of the combinations of α, ζ, and the estimated mantle viscosity. The tidal quality factor is a frequency-dependent quantity inversely proportional to the rate of energy dissipation caused by tidal loading (for a proper definition, see, e.g., Efroim-

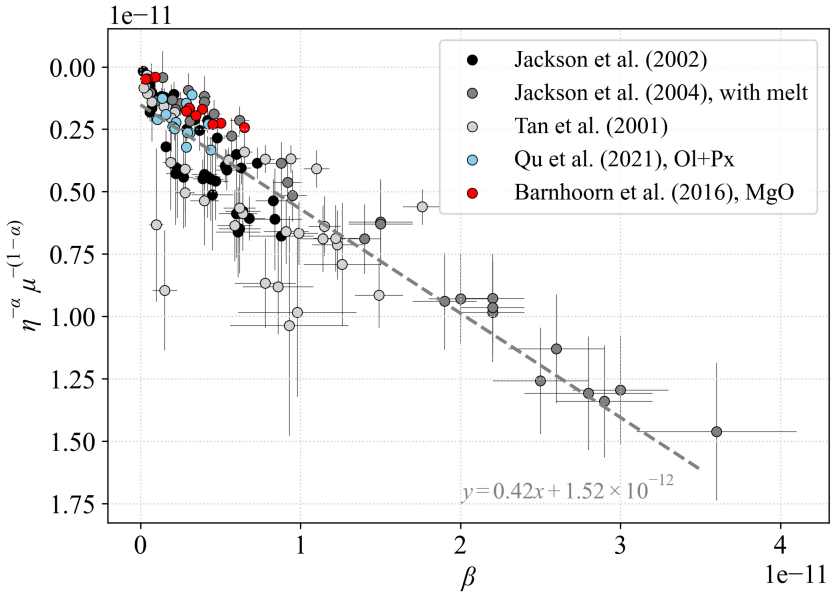

Figure 3. A variation on Figure 4 of Castillo-Rogez et al. (2011), with added data points from Jackson et al. (2004), Barnhoorn et al. (2016), and Qu et al. (2021). The gray dashed line indicates a linear fit to all data with $R^2 = 0.76$.

sky, 2012a, 2012b), which might provide additional insight into the rheology of celestial bodies. It has been estimated for the Moon from lunar laser ranging (LLR; e.g., Williams & Boggs, 2015), for Mars from the rate of Phobian orbital evolution (e.g., Lainey et al., 2007), and under certain assumptions on the surface-atmosphere coupling, it can also be calculated for Venus from the equilibrium of the solid-body and atmospheric tides (Correia et al., 2003). In Figure 4 and in the following Figures 5-6, we specifically highlight the value 38 ± 4 derived at the monthly period for the Moon (Williams & Boggs, 2015).

As we can see in Figures 4-6, for ζ between 0.1 and 1, the inferred mantle viscosity only varies by one order of magnitude. This is true for all four considered bodies. The influence of α for typical values between 0.15 and 0.4 is much more pronounced, and varies among the planets. For Venus and Mercury, the influence is comparatively small at 1 to 3 orders of magnitude, for Mars and the Moon, it is 4 to 6 orders of magnitude.

If the tidal quality factor Q is estimated together with k_2 (at least at the main tidal frequency), it can help to further constrain not only the mantle viscosity but also the parameters of the rheological model assumed for the mantle. As illustrated in Figures 4-6 and emphasised specifically for the Moon, the measurement of Q is able to put tight constraints on the Andrade parameter α. For a lunar Q at the monthly frequency, $Q = 38 \pm 4$ (Williams & Boggs, 2015), the parameter α can be constrained between 0.15 and 0.22. This in turn allows the range of estimated mantle viscosities to be narrowed from $4-6$ to $2-3$ orders of magnnitude (for a fixed ζ). However, the existing measurement of Q does not add almost any information about the parameter ζ. For a fixed core size and for an estimated pair of k_2 and Q at a single frequency, there is always a trade-off between the mantle viscosity η and the parameter ζ (see also Walterová et al., 2023). Potential further information on the rheology of planetary mantles can be obtained from tidal measurements at multiple frequencies (Williams & Boggs, 2015; Bagheri et al., 2019; Cascioli et al., 2023).

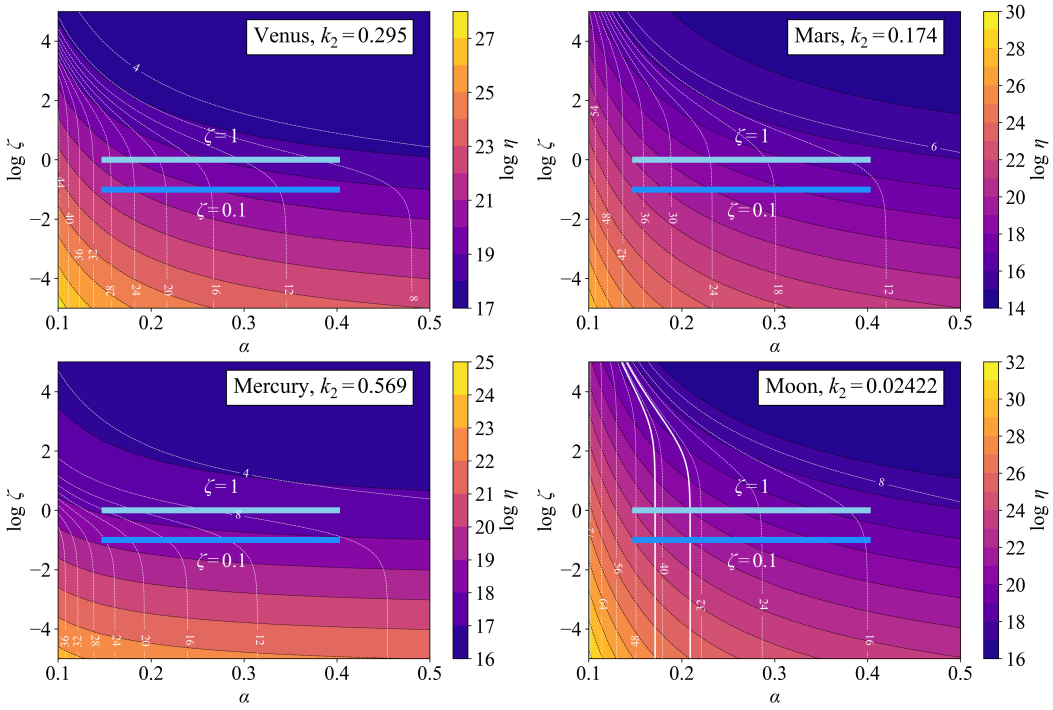

Figure 4. Effect of the Andrade parameters α and ζ on the inferred mantle viscosity (color-coded) corresponding to the mean values of the empirical tidal Love numbers k_2 for four terrestrial bodies: Venus, Mars, Mercury, and the Moon. The core radius is assumed constant and the core is modelled as a fluid of low viscosity (1 Pa s). Solid horizontal bars indicate the typical values of α, for two realistic choices of ζ: 0.1 (following Figure 3) and 1 (following Castillo-Rogez et al., 2011). The thin white dotted lines are the isolines of tidal quality factor Q corresponding to the combination of α, ζ, and η at the main tidal frequency. Specifically, the range of Q estimated for the Moon from LLR (Williams & Boggs, 2015) is plotted with the solid white lines.

3 Discussion

The parameters α, β, β^*, and ζ of the Andrade rheological model, which are used for the interpretation of geodetic measurements, are usually assumed based on the existing experiments. For this reason, it is essential that samples of different compositions are studied and that the effect of high confining pressures, relatively high temperatures, and low-frequency loading with low stress amplitudes are investigated. Despite dedicated efforts in measuring the frequency-dependent response of planet-forming materials, and despite the advances in rheological experiments under high confining pressures (Li & Weidner, 2007), the modelling of tidal deformation of terrestrial planets relies on the extrapolation of the laboratory results to the planet's interior conditions. While it is well established that the viscosity of a homogeneous material scales with pressure and temperature following the Arrhenius law (and with grain size and water content following the power law; e.g., Hirth & Kohlstedt, 2003), and the Andrade parameter β scales in the same way, the parameter dependence of α and ζ is not well known. To our knowledge, the only work dealing with the parameter dependence of α is the paper by Lee et al. (2011), who illustrate its relation to the grain shape and the loading frequency. Specifically, α should be related to the stress singularities at grain triple junctions (Lee et al., 2011; Picu & Gupta, 1996).

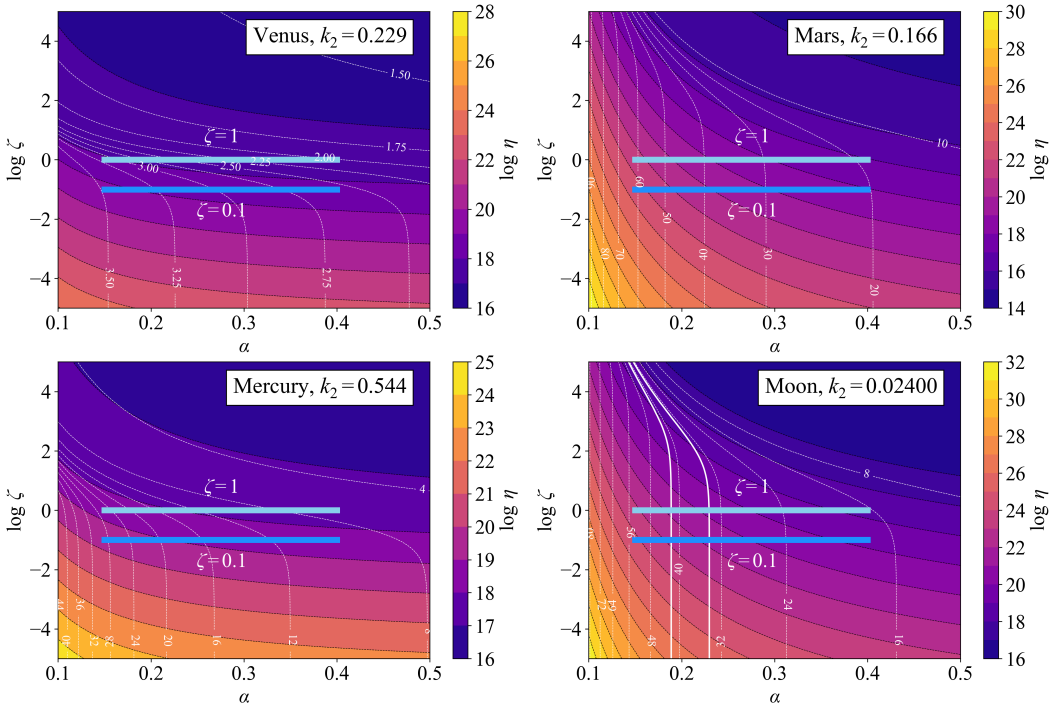

Figure 5. Same as Figure 4, but for the lower bound of the Love numbers reported in the literature. Note that for the considered core radius of 3147 km, the lower bound on the k_2 of Venus cannot be fitted by any model with a fully liquid core (see also Dumoulin et al., 2017). Therefore, in this specific case, we modelled the Cytherean core as fully solid, with $\eta_{\text{core}} = 10^{17}$ Pa s and $\mu_{\text{core}} = 150$ GPa.

As we have seen in Figure 1, the parameters α and ζ depend mildly on the sample's rigidity—and their rigidity-dependence might also be a function of the composition. Moreover, the exponent of the anelastic term, α, fitted to the laboratory data, apparently depends on the experimental method: for microcreep experiments, it is higher than for torsional oscillations and it exhibits a tendency to increase with sample rigidity. The difference likely results from the data processing, where the time-domain measurements of microcreep are first fitted with the original Andrade law with $\alpha = 1/3$ and only then transformed to the frequency domain. Tan et al. (2001) notes that the fitting of microcreep data "involves a hierarchy of assumptions and/or approximations" and that the torsional oscillation data should be considered more qualitatively robust. The parameter ζ for olivine samples slightly increases with rigidity, independent of the method. For MgO, ζ also increases with rigidity but the trend is weaker than for olivine and sample-dependent. Typically, ζ of olivine, Ol-Px mixtures, and MgO falls between 0.01 and 100 (Figure 2); the two data points from Tan et al. (2001) that exhibit a considerably higher ζ are suspected to be outliers.

We note that the data for pure olivine of either natural or synthetic origin, adopted from the discussed papers, were collected in the rigidity range from ~ 20 to ~ 70 GPa. While this range might be sufficient for smaller bodies (the Moon, Mercury, and Mars), the dependence of α and ζ on rigidity is not explored sufficiently for the rigidities relevant to deep Cytherean or terrestrial interior. The mantles of Earth-sized or Venus-sized planets can reach rigidities as high as 200 GPa close to the core-mantle boundary and since the tidal dissipation of bodies with a liquid outer core (or with a fully liquid core) is greatest in the lower mantle (see, e.g., Tobie et al., 2005; Henning & Hurford, 2014),

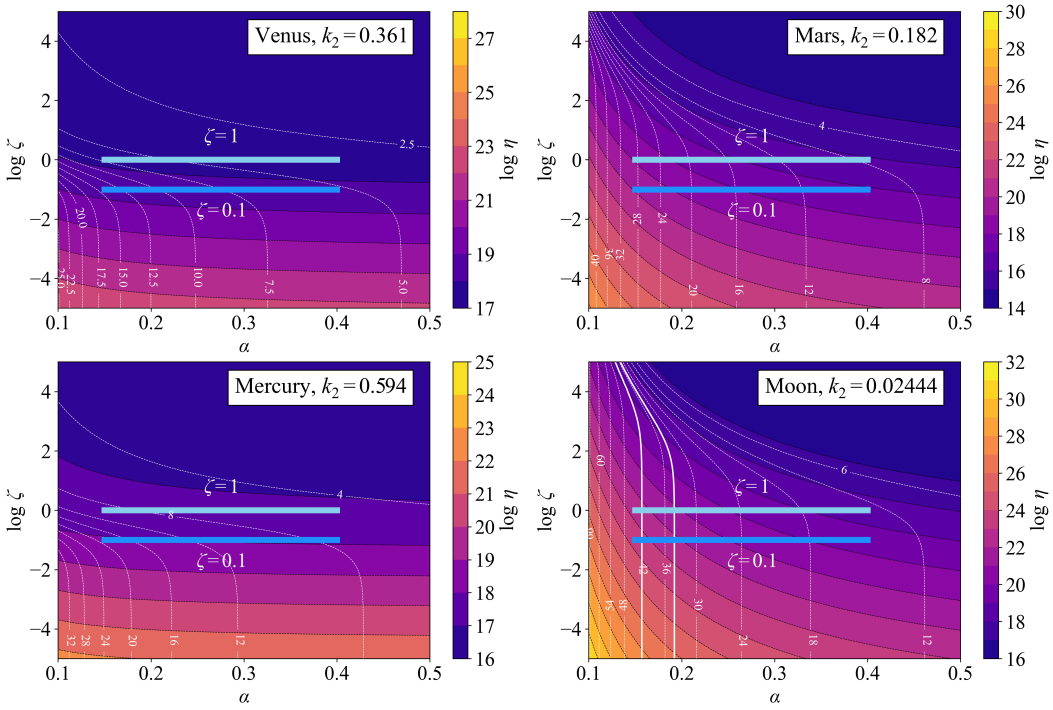

Figure 6. Same as Figure 4, but for the upper bound of the Love numbers reported in the literature.

the rheological parameters of samples with high unrelaxed rigidity are of major interest. If ζ increases with rigidity, as is tentatively indicated in Figure 1b, the viscous term in the dynamic compliance of the Andrade model (equation (15)) might have a strong impact on the tidal deformation of large terrestrial planets.

In that regard, to understand the effect of the depth dependence of the parameter ζ, we considered the Venus model from Section 2.2 with three different assumptions on the radial dependence of ζ: one with a constant $\zeta = 1$ in the entire mantle, one with ζ decreasing logarithmically from 100 at the core-mantle boundary to 0.01 under the crust, and the third one with ζ increasing within the same interval (Figure 7). The second case, ζ decreasing with radius, is consistent with the expected dependence of ζ on μ mentioned in the previous paragraph. For a fixed mantle viscosity $\eta = 10^{20}$ Pa s and a fixed core size, the decrease of ζ with radius results in a difference smaller than 0.01 in the predicted k_2 with respect to a depth-independent $\zeta = 1$. The greatest difference in Q is approximately 10. The (less realistic) increase of ζ with radius results in more pronounced differences, up to 0.02 in k_2 and over 30 in Q. Although the variable ζ changes the predicted k_2 by less than 5%, it should be considered as one of the contributions to the uncertainties of the interior structure parameters.

In the two previous paragraphs, we only referred to the properties of olivine. For the sake of tidal modeling, it is typically assumed that the mantle of terrestrial planets follows the same rheological law as pure olivine. Then, either the $\alpha - \beta$ parameterisation with a pseudo-frequency master variable is used (with the parameters obtained for sample 6585 of Jackson & Faul, 2010) or the $\alpha - \zeta$ parameterisation with $\zeta \approx 1$ fitted to olivine data of Tan et al. (2001) and Jackson et al. (2002) is applied (Castillo-Rogez et al., 2011). The first approach has been used, e.g., for the study of Mercury (Padovan et al., 2014; Steinbrügge et al., 2018; Goossens et al., 2022), Mars (Plesa et al., 2018; Bagheri

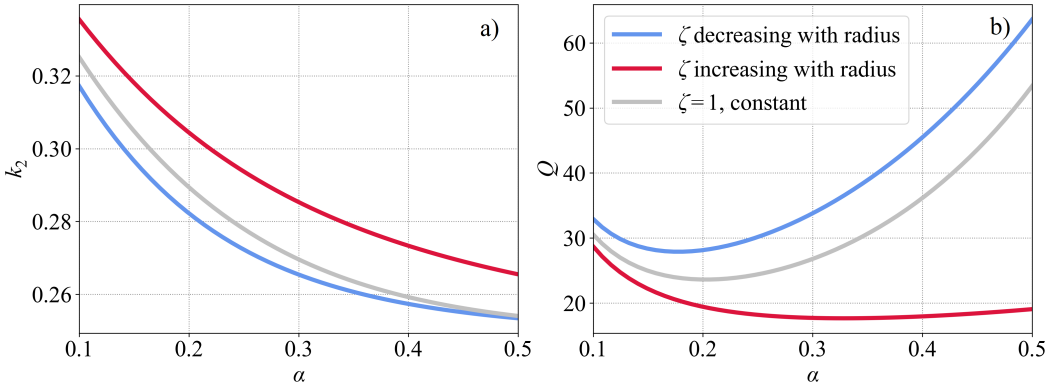

Figure 7. Predicted tidal Love number k_2 (left) and tidal quality factor Q (right) for a model of Venus with mantle viscosity $\eta = 10^{20}$ Pa s, a liquid core of radius 3147 km, and the elastic profile given by rescaled PREM (Dziewonski & Anderson, 1981). The parameter ζ is considered either constant ($\zeta = 1$) or decreasing/increasing logarithmically with depth in the interval $[0.01, 100]$.

et al., 2019), and the Moon (Xiao et al., 2022). The second approach or its equivalent with the implicit assumption of $\zeta = 1$ has been used for icy moons (e.g., Castillo-Rogez et al., 2011; Běhounková et al., 2013), Venus (Dumoulin et al., 2017; Bolmont et al., 2020; Xiao et al., 2021; Saliby et al., 2023), for the Moon (Xiao et al., 2022), and in exoplanetary studies (e.g., Renaud & Henning, 2018; Bolmont et al., 2020). The α–ζ approach with $\zeta = 1$ (Castillo-Rogez et al., 2011) is also implemented in the tidal software ALMA[3] (Melini et al., 2022).

However, it has been argued by Barnhoorn et al. (2016), based on the experiments of Girard et al. (2016), that the viscoelastic deformation and dissipation in the deep mantle of the Earth might be governed by the processes in ferropericlase (containing MgO) rather than by the more abundant silicate perovskite. If this is the case, a change in the temperature and pressure dependence of the rheological parameters used for tidal modeling of large terrestrial planets like the Earth and Venus might be required.

We also analyzed the traditional assumption of $\zeta \approx 1$. Interestingly, for the two melt-free olivine datasets of Tan et al. (2001) and Jackson et al. (2002), we found a linear dependence of $\eta^{-\alpha}\mu^{-(1-\alpha)}$ on the original Andrade parameter β in the form:

$$\eta^{-\alpha}\mu^{-(1-\alpha)} = 0.54\beta + 1.57 \times 10^{-12}. \tag{19}$$

The slope of this dependence is, by definition, equal to ζ^{α}. For $\alpha = 0.2 - 0.3$, we obtain $\zeta = 0.05$–0.13, a value that is about an order of magnitude smaller than implied by the fit of Castillo-Rogez et al. (2011). When considering the data points for all samples used in this work (independent of composition and melt fraction), we obtain $\zeta = 0.01 - 0.06$. The median value of ζ calculated individually for each of the data points (i.e., using the true α for each of the data points) is $\zeta = 0.33$. Nevertheless, the assumption of $\zeta = 1$ is not incorrect: as illustrated in Figures 1b and 2, it falls approximately in the middle of the interval of permissible ζ.

Figures 4-6 show that varying the considered values of α and ζ has profound effects on the inferred mantle viscosity of our toy-model terrestrial planets with a prescribed tidal Love number k_2 (see also Dumoulin et al., 2017; Renaud & Henning, 2018). Increasing α or ζ leads to lower predicted mantle viscosity. Ideally, estimating the Andrade parameters α and ζ (or α and β, in the original parameterisation) should be incorporated

into the interior structure inversion (as is done, e.g., in Bagheri et al., 2019; Xiao et al., 2022). Additional information can be obtained by measuring the tidal quality factor Q, which helps to narrow the interval of estimated α. Possible future measurements of a planet's response at multiple loading frequencies might also reveal the need for more complex rheological models than Andrade's law (Williams & Boggs, 2015; Lau & Faul, 2019).

For the calculations presented in Figures 4-6, we considered the planetary mantles fully solid, following the rigidity and density structure prescribed by rescaled PREM or by VPREMOON, and having a constant viscosity. The presence of any low-viscosity, possibly partially molten layers anywhere in the mantle would presumably imply different (higher) viscosities in the rest of the mantle (e.g., Bolmont et al., 2020). Additionally, for Figure 5, showing the mantle viscosity for the lowest value of the k_2 interval presented in the literature, we assumed that the core of Venus is fully solid. For the Love number in question, and for the prescribed mantle structure and core size, it was impossible to find a solution with a fully liquid core. However, the rheological parameters of a fully solid core also affect the resulting tidal response, and they deserve a mention. We chose the parameters $\eta_{\mathrm{core}} = 10^{17}\,\mathrm{Pa\,s}$ and $\mu_{\mathrm{core}} = 150\,\mathrm{GPa}$. With a lower core viscosity, it is already impossible to fit the prescribed k_2. With a higher core viscosity, we observe a preference for a lower viscosity of the mantle and higher predicted Q. Similarly, increasing the rigidity of the core from 150 GPa to 300 GPa results in lower inferred mantle viscosities.

Within the k_2 error bounds given in the literature, the predicted mantle viscosity of the individual planets varies by different amounts. The effect of α and ζ on these variations is depicted in Figure 8. For the k_2 values measured so far, including the error, the uncertainty in viscosity is smallest for Venus and the Moon and is at most one order of magnitude. Interestingly, the error in the inferred viscosity is the greatest for Mars (up to 4 orders of magnitude), although the k_2 of Mars is known much more precisely than that of Venus (4% uncertainty in comparison to 20% uncertainty). It is important to note that for this estimate, we assume that the core size is known. Still, this example shows that the inference of Cytherean mantle viscosity can be relatively accurate even with previously unconstrained Andrade parameters. With a higher ζ or α, the response of a body governed by the Andrade rheology resembles the response of a planet described by the Maxwell rheology, for which the sensitivity of k_2 to mantle viscosity is weaker.

In Section 2.1, we also presented new Andrade fits to the two datasets that were not analysed in the context of this rheological model before (Barnhoorn et al., 2016; Qu et al., 2021). It is worth noting that while the fitted parameters α, β^*, and μ, listed in the online material, are relatively robust with respect to the optimization step size and our choice of the cost function, the sample viscosity η is extremely sensitive to the optimization scheme used. This also affects the derived values of ζ that can vary by orders of magnitude. The most consistent results are obtained from fitting to the samples studied under the highest temperatures ($1100 - 1300\,^{\circ}\mathrm{C}$). We adjust the optimization parameters to values that predict viscosity monotonically decreasing with temperature for the entire temperature range considered. Furthermore, we do not use data corresponding to temperatures lower than $1100\,^{\circ}\mathrm{C}$ because at lower temperatures, the dissipation spectrum might already contain additional dissipation peaks (Webb & Jackson, 2003; Jackson & Faul, 2010; Sundberg & Cooper, 2010). We also disregard the viscosity and ζ predictions for cases where viscosity cannot be fitted uniquely. This happens when the laboratory data at a given temperature and for a given composition only cover the interval of frequencies at which the sample reacts almost purely anelastically. Nevertheless, parameters α and β (or β^*) of those samples could still be fitted.

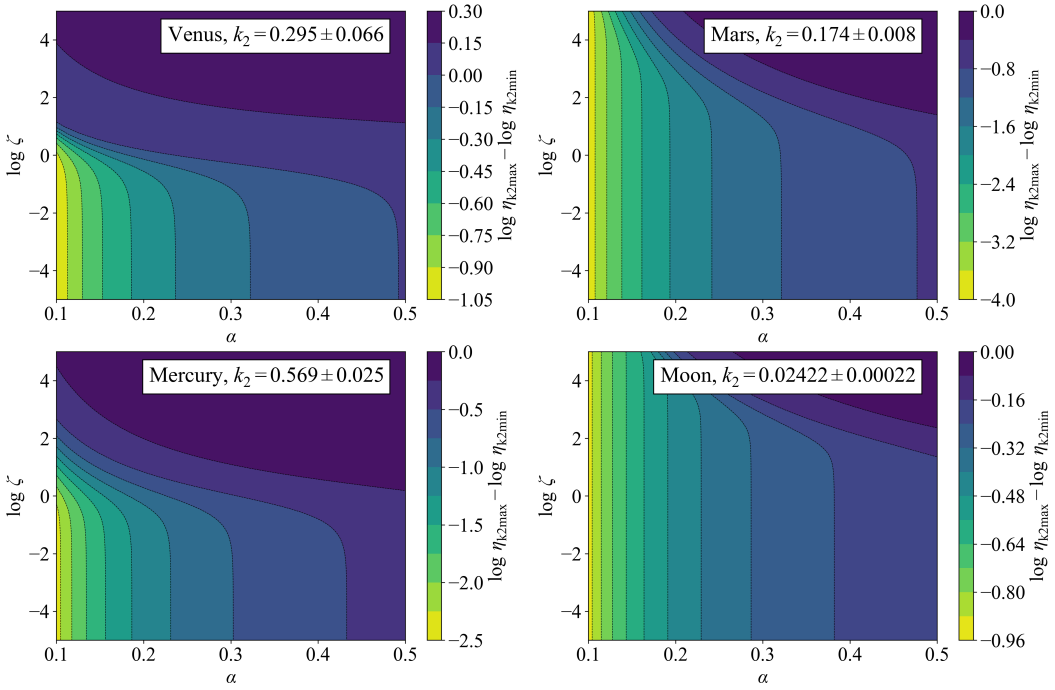

Figure 8. The difference between mantle viscosity predicted for the upper bound of the k_2 interval and the mantle viscosity predicted for the lower bound of the k_2 interval presented in the literature for three terrestrial planets and the Moon. Effect of Andrade parameters α and ζ.

4 Conclusions

When interpreting the measurements of tidal deformation of planets and satellites in the Solar System, an assumption on the solid body's rheological behavior is often required. The dependence of the rheology on temperature, pressure, and grain size then provides a link between the measured quantities and the planet's interior structure, thermal state, or even thermal history. In this work, we discussed two parameterisations of the popular Andrade rheological model and provided a review of the rheological parameters available in the literature. When necessary, we derived the values of the parameters from the measured quantities.

In Figures 1-3, we illustrated the dependence of empirical parameters α and ζ on the rigidity, the relation between the characteristic time scales of the viscous and anelastic relaxation, and we also attempted to extend the fit of Castillo-Rogez et al. (2011) to newer datasets. For these analyses, the high-pressure deformation and attenuation data for olivine (Tan et al., 2001; Jackson et al., 2002, 2004), Ol+Px mixtures (Qu et al., 2021), and MgO (Barnhoorn et al., 2016) were used. We found that the parameter ζ is mildly rigidity-dependent; the typical values of α are $0.15 - 0.4$, and the values of ζ fall into the interval $0.01 - 100$. The median value of ζ is 0.33.

The uncertainties in the Andrade parameters then affect the inferred interior properties of terrestrial planets and rocky moons. Focusing specifically on the tidal effective mantle viscosity (Figures 4-8), we saw that, depending on the planet considered, the increase of α from 0.15 to 0.4 might decrease the predicted viscosity by up to six orders of magnitude. The increase of ζ by one order of magnitude leads to the decrease of the predicted viscosity by one order of magnitude for all discussed planets. Additional information about mantle viscosity and the Andrade parameter α can be obtained by measuring the tidal quality factor Q. On the other hand, the parameter ζ cannot be easily

constrained by single-frequency k_2 and Q: there is a trade-off between ζ and the mantle viscosity. A possible remedy to this problem would be a precise estimation of tidal response at multiple frequencies (e.g., Bagheri et al., 2019).

Our results are based on a limited number of datasets that are currently available to the tidal modelling community. Nevertheless, they show several regularities that should be taken into account in tidal modelling and in the inversion of geodetic measurements. The uncertainty in the rheological parameters may have greater influence on the determination of mantle viscosities than the uncertainty of k_2. We believe that a better understanding of the parameter dependencies of α, ζ, and β (or β^*), including the effect of temperature, composition, grain size, sample rigidity, and (reference) viscosity will help to acquire a clearer picture of the interior structure of terrestrial worlds in the Solar System. In view of the current or upcoming missions to the planets where most information about the interior is obtained from the geodetic (including tidal) measurements and where the opportunity for seismic measurements is limited (Mercury and Venus), the study of rheological behaviour of materials under mantle-like conditions promises important improvements to the models.

5 Open Research

The preliminary version of the software and data used in this study is available in the repository of the corresponding author: `https://github.com/kanovami/AndradeParameters`. The final and complete version, as well as the DOI, will be provided during the review process.

Acknowledgments

We would like to thank Prof. Ian Jackson for sharing with us the raw data from the study of Barnhoorn et al. (2016). M.W. and A.C.P. gratefully acknowledge the financial support and endorsement from the DLR Management Board Young Research Group Leader Program and the Executive Board Member for Space Research and Technology. F.W.W. thanks the PUNCH4NFDI consortium (DFG fund NFDI 39/1) for financial support.

References

Anderson, D. L., & Given, J. W. (1982, May). Absorption band Q model for the Earth. *J. Geophys. Res.*, *87*(B5), 3893-3904. doi: 10.1029/JB087iB05p03893

Anderson, D. L., & Minster, J. B. (1979, August). The frequency dependence of Q in the Earth and implications for mantle rheology and Chandler wobble. *Geophysical Journal*, *58*, 431-440. doi: 10.1111/j.1365-246X.1979.tb01033.x

Andrade, E. N. D. C. (1910, June). On the Viscous Flow in Metals, and Allied Phenomena. *Proc. R. Soc. A*, *84*(567), 1-12.

Bagheri, A., Efroimsky, M., Castillo-Rogez, J., Goossens, S., Plesa, A.-C., Rambaux, N., ... Giardini, D. (2022, August). Tidal insights into rocky and icy bodies: an introduction and overview. *Advances in Geophysics*, *63*, 231-320. doi: 10.1016/bs.agph.2022.07.004

Bagheri, A., Khan, A., Al-Attar, D., Crawford, O., & Giardini, D. (2019, November). Tidal Response of Mars Constrained From Laboratory-Based Viscoelastic Dissipation Models and Geophysical Data. *Journal of Geophysical Research (Planets)*, *124*(11), 2703-2727. doi: 10.1029/2019JE006015

Barnhoorn, A., Jackson, I., Fitz Gerald, J. D., Kishimoto, A., & Itatani, K. (2016, July). Grain size-sensitive viscoelastic relaxation and seismic properties of polycrystalline MgO. *Journal of Geophysical Research (Solid Earth)*, *121*(7), 4955-4976. doi: 10.1002/2016JB013126

Bass, J. D. (1995). Elasticity of minerals, glasses, and melts. In *Mineral physics & crystallography* (p. 45-63). American Geophysical Union (AGU). doi: 10.1029/

RF002p0045

Berckhemer, H., Kampfmann, W., Aulbach, E., & Schmeling, H. (1982, July). Shear modulus and Q of forsterite and dunite near partial melting from forced-oscillation experiments. *Physics of the Earth and Planetary Interiors*, *29*(1), 30-41. doi: 10.1016/0031-9201(82)90135-2

Bingham, E. C., & Reiner, M. (1933, March). The Rheological Properties of Cement and Cement-Mortar-Stone. *Physics*, *4*(3), 88-96. doi: 10.1063/1.1745167

Bolmont, E., Breton, S. N., Tobie, G., Dumoulin, C., Mathis, S., & Grasset, O. (2020, December). Solid tidal friction in multi-layer planets: Application to Earth, Venus, a Super Earth and the TRAPPIST-1 planets. Potential approximation of a multi-layer planet as a homogeneous body. *Astron. Astrophys.*, *644*, A165. doi: 10.1051/0004-6361/202038204

Braun, M. L. (1936, November). A Preliminary Study of the After-Effect or Drift in Rubber Under Constant Load. *Physics*, *7*(11), 421-425. doi: 10.1063/1.1745352

Běhounková, M., Tobie, G., Choblet, G., & Čadek, O. (2013, September). Impact of tidal heating on the onset of convection in Enceladus's ice shell. *Icarus*, *226*(1), 898-904. doi: 10.1016/j.icarus.2013.06.033

Cascioli, G., Renaud, J. P., Mazarico, E., Durante, D., Iess, L., Goossens, S., & Smrekar, S. (2023, April). Constraining the Venus Interior Structure with Future VERITAS Measurements of the Gravitational Atmospheric Loading. *Planet. Sci. J.*, *4*(4), 65. doi: 10.3847/PSJ/acc73c

Castillo-Rogez, J. C., Efroimsky, M., & Lainey, V. (2011, September). The tidal history of Iapetus: Spin dynamics in the light of a refined dissipation model. *J. Geophys. Res. Planets*, *116*(E9), E09008. doi: 10.1029/2010JE003664

Correia, A. C. M., Laskar, J., & de Surgy, O. N. (2003, May). Long-term evolution of the spin of Venus. I. theory. *Icarus*, *163*(1), 1-23. doi: 10.1016/S0019-1035(03)00042-3

Cottrell, A. H., & Aytekin, V. (1947, September). Andrade's Creep Law and the Flow of Zinc Crystals. *Nature*, *160*(4062), 328-329. doi: 10.1038/160328a0

Dorn, J. (1955). Some fundamental experiments on high temperature creep. *Journal of the Mechanics and Physics of Solids*, *3*(2), 85-116. doi: 10.1016/0022-5096(55)90054-5

Dumoulin, C., Tobie, G., Verhoeven, O., Rosenblatt, P., & Rambaux, N. (2017, June). Tidal constraints on the interior of Venus. *J. Geophys. Res. Planets*, *122*(6), 1338-1352. doi: 10.1002/2016JE005249

Dziewonski, A. M., & Anderson, D. L. (1981, June). Preliminary reference Earth model. *Phys. Earth Planet. Inter.*, *25*(4), 297-356. doi: 10.1016/0031-9201(81)90046-7

Efroimsky, M. (2012a). Bodily tides near spin-orbit resonances. *Celest. Mech. Dyn. Astron.*, *112*(3), 283-330. doi: 10.1007/s10569-011-9397-4

Efroimsky, M. (2012b). Tidal Dissipation Compared to Seismic Dissipation: In Small Bodies, Earths and Super-Earths. *Astrophys. J.*, *746*(2), 150. doi: 10.1088/0004-637X/746/2/150

Efroimsky, M., & Lainey, V. (2007, December). Physics of bodily tides in terrestrial planets and the appropriate scales of dynamical evolution. *Journal of Geophysical Research (Planets)*, *112*(E12), E12003. doi: 10.1029/2007JE002908

Filon, L. N. G., & Jessop, H. T. (1923, January). On the Stress-Optical Effect in Transparent Solids Strained beyond the Elastic Limit. *Philosophical Transactions of the Royal Society of London Series A*, *223*, 89-125. doi: 10.1098/rsta.1923.0003

Gailus, W. J., & Telfair, D. (1945). Creep properties of molded phenolic plastics at elevated temperatures. *Trans. A.S.M.E.*, *67*(4), 253-258.

Garcia, R. F., Gagnepain-Beyneix, J., Chevrot, S., & Lognonné, P. (2011, September). Very preliminary reference Moon model. *Physics of the Earth and Plan-*

etary Interiors, *188*(1), 96-113. doi: 10.1016/j.pepi.2011.06.015

Genova, A., Goossens, S., Mazarico, E., Lemoine, F. G., Neumann, G. A., Kuang, W., ... Zuber, M. T. (2019, April). Geodetic Evidence That Mercury Has A Solid Inner Core. *Geophys. Res. Lett.*, *46*(7), 3625-3633. doi: 10.1029/2018GL081135

Girard, J., Amulele, G., Farla, R., Mohiuddin, A., & Karato, S.-i. (2016, January). Shear deformation of bridgmanite and magnesiowüstite aggregates at lower mantle conditions. *Science*, *351*(6269), 144-147. doi: 10.1126/science.aad3113

Goossens, S., Renaud, J. P., Henning, W. G., Mazarico, E., Bertone, S., & Genova, A. (2022, February). Evaluation of Recent Measurements of Mercury's Moments of Inertia and Tides Using a Comprehensive Markov Chain Monte Carlo Method. *Planet. Sci. J.*, *3*(2), 37. doi: 10.3847/PSJ/ac4bb8

Gribb, T. T., & Cooper, R. F. (1998, November). Low-frequency shear attenuation in polycrystalline olivine: Grain boundary diffusion and the physical significance of the Andrade model for viscoelastic rheology. *J. Geophys. Res.*, *103*(B11), 27,267-27,279. doi: 10.1029/98JB02786

Gueguen, Y., Darot, M., Mazot, P., & Woirgard, J. (1989, June). Q^{-1} of forsterite single crystals. *Physics of the Earth and Planetary Interiors*, *55*(3-4), 254-258. doi: 10.1016/0031-9201(89)90073-3

Henderson, C. (1951, March). The Application of Boltzmann's Superposition Theory to Materials Exhibiting Reversible β Flow. *Proceedings of the Royal Society of London Series A*, *206*(1084), 72-86. doi: 10.1098/rspa.1951.0057

Henning, W. G., & Hurford, T. (2014, July). Tidal Heating in Multilayered Terrestrial Exoplanets. *Astrophys. J.*, *789*(1), 30. doi: 10.1088/0004-637X/789/1/30

Hirth, G., & Kohlstedt, D. (2003, January). Rheology of the upper mantle and the mantle wedge: A view from the experimentalists. *Washington DC American Geophysical Union Geophysical Monograph Series*, *138*, 83-105. doi: 10.1029/138GM06

Jackson, I. (2000, January). Laboratory measurement of seismic wave dispersion and attenuation: Recent progress. *Washington DC American Geophysical Union Geophysical Monograph Series*, *117*, 265-289. doi: 10.1029/GM117p0265

Jackson, I., & Faul, U. H. (2010). Grainsize-sensitive viscoelastic relaxation in olivine: Towards a robust laboratory-based model for seismological application. *Phys. Earth Planet. Inter.*, *183*(1), 151-163. (Special Issue on Deep Slab and Mantle Dynamics) doi: 10.1016/j.pepi.2010.09.005

Jackson, I., Faul, U. H., Fitz Gerald, J. D., & Tan, B. H. (2004, June). Shear wave attenuation and dispersion in melt-bearing olivine polycrystals: 1. Specimen fabrication and mechanical testing. *Journal of Geophysical Research (Solid Earth)*, *109*(B6), B06201. doi: 10.1029/2003JB002406

Jackson, I., Fitz Gerald, J. D., Faul, U. H., & Tan, B. H. (2002, December). Grain-size-sensitive seismic wave attenuation in polycrystalline olivine. *J. Geophys. Res. Solid Earth*, *107*(B12), 2360. doi: 10.1029/2001JB001225

Jeffreys, H. (1958, March). A Modification of Lomnitz's Law of Creep in Rocks. *Geophysical Journal*, *1*(1), 92-95. doi: 10.1111/j.1365-246X.1958.tb00037.x

Jeffreys, H. (1972, January). Creep in the earth and planets. *Tectonophysics*, *13*, 569-582. doi: 10.1016/0040-1951(72)90038-8

Jeffreys, H., & Crampin, S. (1960, January). Rock creep: a correction. *Mon. Not. R. Astron. Soc.*, *121*, 571. doi: 10.1093/mnras/121.6.571

Johnson, A. E. (1941). The creep recovery of a 0.17 per cent carbon steel. *Proceedings of the Institution of Mechanical Engineers*, *145*(1), 210-220. doi: 10.1243/PIME_PROC_1941_145_042_02

Karato, S., & Spetzler, H. A. (1990, November). Defect microdynamics in minerals and solid state mechanisms of seismic wave attenuation and velocity dispersion in the mantle. *Reviews of Geophysics*, *28*(4), 399-421. doi: 10.1029/RG028i004p00399

Kê, T.-S. (1947, April). Experimental Evidence of the Viscous Behavior of Grain Boundaries in Metals. *Physical Review*, *71*(8), 533-546. doi: 10.1103/PhysRev.71.533

Kennedy, A. J. (1953, April). On the generality of the cubic creep function. *Journal of Mechanics Physics of Solids*, *1*(3), 172-181. doi: 10.1016/0022-5096(53)90035-0

Kennedy, A. J. (1956, May). A reconciliation of certain recovery properties in metals. *Journal of Mechanics Physics of Solids*, *4*(3), 162-166. doi: 10.1016/0022-5096(56)90071-0

Khan, A., Liebske, C., Rozel, A., Rivoldini, A., Nimmo, F., Connolly, J. A. D., ... Giardini, D. (2018, February). A Geophysical Perspective on the Bulk Composition of Mars. *Journal of Geophysical Research (Planets)*, *123*(2), 575-611. doi: 10.1002/2017JE005371

Konopliv, A. S., Park, R. S., Rivoldini, A., Baland, R.-M., Le Maistre, S., Van Hoolst, T., ... Dehant, V. (2020, November). Detection of the Chandler Wobble of Mars From Orbiting Spacecraft. *Geophys. Res. Lett.*, *47*(21), e90568. doi: 10.1029/2020GL090568

Konopliv, A. S., & Yoder, C. F. (1996, January). Venusian k_2 tidal Love number from Magellan and PVO tracking data. *Geophys. Res. Lett.*, *23*(14), 1857-1860. doi: 10.1029/96GL01589

Lainey, V., Dehant, V., & Pätzold, M. (2007, April). First numerical ephemerides of the Martian moons. *Astron. Astrophys.*, *465*(3), 1075-1084. doi: 10.1051/0004-6361:20065466

Lau, H. C. P., & Faul, U. H. (2019, February). Anelasticity from seismic to tidal timescales: Theory and observations. *Earth and Planetary Science Letters*, *508*, 18-29. doi: 10.1016/j.epsl.2018.12.009

Lee, L. C., Morris, S. J. S., & Wilkening, J. (2011, June). Stress concentrations, diffusionally accommodated grain boundary sliding and the viscoelasticity of polycrystals. *Proceedings of the Royal Society of London Series A*, *467*(2130), 1624-1644. doi: 10.1098/rspa.2010.0447

Li, L., & Weidner, D. J. (2007, May). Energy dissipation of materials at high pressure and high temperature. *Review of Scientific Instruments*, *78*(5), 053902-053902-8. doi: 10.1063/1.2735587

Melini, D., Saliby, C., & Spada, G. (2022, December). On computing viscoelastic Love numbers for general planetary models: the ALMA^3 code. *Geophysical Journal International*, *231*(3), 1502-1517. doi: 10.1093/gji/ggac263

Nimmo, F., & Faul, U. H. (2013, December). Dissipation at tidal and seismic frequencies in a melt-free, anhydrous Mars. *Journal of Geophysical Research (Planets)*, *118*(12), 2558-2569. doi: 10.1002/2013JE004499

Nimmo, F., Faul, U. H., & Garnero, E. J. (2012, September). Dissipation at tidal and seismic frequencies in a melt-free Moon. *Journal of Geophysical Research (Planets)*, *117*(E9), E09005. doi: 10.1029/2012JE004160

O'Neill, C. (2021, September). End-Member Venusian Core Scenarios: Does Venus Have an Inner Core? *Geophys. Res. Lett.*, *48*(17), e95499. doi: 10.1029/2021GL095499

Padovan, S., Margot, J.-L., Hauck, S. A., Moore, W. B., & Solomon, S. C. (2014, April). The tides of Mercury and possible implications for its interior structure. *Journal of Geophysical Research (Planets)*, *119*(4), 850-866. doi: 10.1002/2013JE004459

Picu, C. R., & Gupta, V. (1996). Stress singularities at triple junctions with freely sliding grains. *International Journal of Solids and Structures*, *33*(11), 1535-1541. doi: 10.1016/0020-7683(95)00112-3

Plesa, A. C., Padovan, S., Tosi, N., Breuer, D., Grott, M., Wieczorek, M. A., ... Banerdt, W. B. (2018, November). The Thermal State and Interior Structure of Mars. *Geophys. Res. Lett.*, *45*(22), 12,198-12,209. doi:

10.1029/2018GL080728

Qu, T., Jackson, I., & Faul, U. H. (2021, October). Low-Frequency Seismic Properties of Olivine-Orthopyroxene Mixtures. *Journal of Geophysical Research (Solid Earth)*, *126*(10), e2021JB022504. doi: 10.1029/2021JB022504

Renaud, J. P., & Henning, W. G. (2018). Increased Tidal Dissipation Using Advanced Rheological Models: Implications for Io and Tidally Active Exoplanets. *Astrophys. J.*, *857*(2), 29. doi: 10.3847/1538-4357/aab784

Saal, R. N. J., & Labout, J. W. A. (1940). Rheological properties of asphaltic bitumen. *The Journal of Physical Chemistry*, *44*(2), 149-165. doi: 10.1021/j150398a002

Saliby, C., Fienga, A., Briaud, A., Mémin, A., & Herrera, C. (2023, July). Viscosity contrasts in the Venus mantle from tidal deformations. *Planet. Space Sci.*, *231*, 105677. doi: 10.1016/j.pss.2023.105677

Schofield, R. K., & Scott Blair, G. W. (1933, March). The Relationship between Viscosity, Elasticity and Plastic Strength of a Soft Material as Illustrated by Some Mechanical Properties of Flour Dough. II. *Proceedings of the Royal Society of London Series A*, *139*(839), 557-566. doi: 10.1098/rspa.1933.0038

Siebenbürger, M., Ballauff, M., & Voigtmann, T. (2012, Jun). Creep in colloidal glasses. *Phys. Rev. Lett.*, *108*, 255701. doi: 10.1103/PhysRevLett.108.255701

Smith, M. L., & Dahlen, F. A. (1981, January). The period and Q of the Chandler wobble. *Geophysical Journal*, *64*, 223-281. doi: 10.1111/j.1365-246X.1981.tb02667.x

Stähler, S. C., Khan, A., Banerdt, W. B., Lognonné, P., Giardini, D., Ceylan, S., ... Smrekar, S. E. (2021, July). Seismic detection of the martian core. *Science*, *373*(6553), 443-448. doi: 10.1126/science.abi7730

Steinbrügge, G., Padovan, S., Hussmann, H., Steinke, T., Stark, A., & Oberst, J. (2018, October). Viscoelastic Tides of Mercury and the Determination of its Inner Core Size. *Journal of Geophysical Research (Planets)*, *123*(10), 2760-2772. doi: 10.1029/2018JE005569

Sundberg, M., & Cooper, R. F. (2010, July). A composite viscoelastic model for incorporating grain boundary sliding and transient diffusion creep; correlating creep and attenuation responses for materials with a fine grain size. *Philosophical Magazine*, *90*(20), 2817-2840. doi: 10.1080/14786431003746656

Tan, B. H., Jackson, I., & Fitz Gerald, J. D. (1997, May). Shear wave dispersion and attenuation in fine-grained synthetic olivine aggregates: Preliminary results. *Geophys. Res. Lett.*, *24*(9), 1055-1058. doi: 10.1029/97GL00860

Tan, B. H., Jackson, I., & Fitz Gerald, J. D. (2001, January). High-temperature viscoelasticity of fine-grained polycrystalline olivine. *Physics and Chemistry of Minerals*, *28*(9), 641-664. doi: 10.1007/s002690100189

Tobie, G., Mocquet, A., & Sotin, C. (2005, October). Tidal dissipation within large icy satellites: Applications to Europa and Titan. *Icarus*, *177*(2), 534-549. doi: 10.1016/j.icarus.2005.04.006

Walterová, M., Běhounková, M., & Efroimsky, M. (2023). Is there a semi-molten layer at the base of the lunar mantle? *Journal of Geophysical Research: Planets*, *128*(7), e2022JE007652. Retrieved from `https://agupubs.onlinelibrary.wiley.com/doi/abs/10.1029/2022JE007652` (e2022JE007652 2022JE007652) doi: https://doi.org/10.1029/2022JE007652

Webb, S., & Jackson, I. (2003, January). Anelasticity and microcreep in polycrystalline MgO at high temperature: an exploratory study. *Physics and Chemistry of Minerals*, *30*(3), 157-166. doi: 10.1007/s00269-003-0299-1

Williams, J. G., & Boggs, D. H. (2015, April). Tides on the Moon: Theory and determination of dissipation. *Journal of Geophysical Research (Planets)*, *120*(4), 689-724. doi: 10.1002/2014JE004755

Williams, J. G., Konopliv, A. S., Boggs, D. H., Park, R. S., Yuan, D.-N., Lemoine, F. G., ... Zuber, M. T. (2014, July). Lunar interior properties from the

GRAIL mission. *Journal of Geophysical Research (Planets)*, *119*(7), 1546-1578. doi: 10.1002/2013JE004559

Xiao, C., Li, F., Yan, J., Gregoire, M., Hao, W., Harada, Y., ... Barriot, J.-P. (2021, July). Possible Deep Structure and Composition of Venus With Respect to the Current Knowledge From Geodetic Data. *Journal of Geophysical Research (Planets)*, *126*(7), e06243. doi: 10.1029/2019JE006243

Xiao, C., Wu, Y., Yan, J., Harada, Y., Zhang, Y., & Li, F. (2022, December). Comparison of the Effects of Different Viscoelastic and Temperature Models on the Theoretical Tidal Response of the Moon. *Journal of Geophysical Research (Planets)*, *127*(12), e2022JE007215. doi: 10.1029/2022JE007215